Modelling and Optimization of Laser Alloyed AISI 422 Stainless Steel Using Taguchi Approach and Response Surface Model (RSM)

O. S. Fatoba[1*], O. S. Adesina[1], G. A. Farotade[1] and A. A. Adediran[2]

[1]*Department of Chemical, Metallurgical and Materials Engineering, Faculty of Engineering and the Built Environment, Tshwane University of Technology, P.M.B. X680, Pretoria, South Africa.*
[2]*Department of Mechanical Engineering, Landmark University, Omu Aran, Kwara State, Nigeria.*

Authors' contributions

This work was carried out in collaboration between all authors. Author OSF designed the study, wrote the protocol, wrote the first draft of the manuscript, performed the statistical analysis and managed analyses of the study. Author OSA analysed, verified and quality checked the data used in the results and discussion. Author GAF gathered the materials needed to write the review, initiated the literature review of this study and analysed the experimental procedure. Author AAA performed the statistical analysis and proofread the final manuscript. This work was proofread and accepted by all authors before submitted for publication.

Original Research Article

ABSTRACT

This research paper demonstrates the application of Taguchi method and Response surface Methodology (RSM) for optimization of alloyed depth in laser alloying of AISI 422 martensitic stainless steel. The experiment was designed and carried out on the basis of standard L_9 Taguchi's orthogonal array in which three laser processing parameters such as laser power, scanning speed and powder feed rate were arranged at three levels. The processing parameters played an important role in the quality of alloyed coating produced and proper control of these processing parameters resulted in quality alloyed depth and hardness property. From the analysis of mean values of variance (ANOVA) and response surface numerical analysis, the significant laser

_____

Corresponding author: E-mail: fatobaolawale@yahoo.com;

processing parameters were indentified. The results showed that laser power and scanning speed are the most significant parameters affecting the alloyed depth of laser surface alloying (LSA), while the influence of powder feed rate is much minimal.

1. INTRODUCTION

Many engineering materials used in industrial conditions are subjected to corrosion, wear and fatigue attack leading to rapid surface degradation of the material [1]. This deterioration of components results in loss of plant efficiency, total shutdown and aggressive damage in a number of industries. It is for these reasons that hard coatings are produced on materials to minimize cost, energy and conserve raw materials [1].

Due to the high mechanical strength and moderate corrosion resistance exhibited by martensitic stainless steels (MSS), they are frequently used in the manufacture of pump propellers, pressure vessels, steam generators, turbines and valves [2]. These steels are mainly of Fe-Cr-C ternary alloy system and they derive strength and ductility from their unique microstructure which can be controlled by heat treatment [3,4]. MSS is an important material due to its remarkable flexibility in metal working and heat treating to produce different mechanical, physical and chemical properties [5]. Nevertheless, their use is restricted because they are prone to pitting corrosion in the presence of chloride ions and have low hardness property [6,7,8]. Failure of MSS during engineering applications due to corrosion, oxidation, friction, fatigue and wear is initiated from the surface because free surface is more prone to environmental degradation, and intensity of externally applied load is often highest at the surface. Therefore, there is increasing interest for improving the surface properties through various surface modification techniques [9,10,11].

Modification of surface properties plays an important role in optimizing a material's performance for a given application. Modern industrial applications require materials with special surface properties such as high hardness, wear and corrosion resistance. Therefore, different industrial sectors need an alternative technique for enhanced surface properties. Laser surface alloying (LSA) has attracted substantial attention in recent years as an efficient method to improve the mechanical

and chemical surface properties of engineering components [12]. The improvement in these properties by the LSA technique is achieved by introducing alloying materials into the laser-melted component surface, usually in the form of powder. The varied choice of alloying materials that can be integrated by this method ensures that the surface properties can be modified to impart good wear, oxidation and corrosion properties [13-15]. The LSA technique for surface modification now has distinctive advantages that are well acknowledged and include the reduction in the grain size as a result of rapid cooling rates and the formation of meta-stable structures that have unique properties [16]. Therefore, optimization of process parameters is one of the most critical stages in the development of an efficient and economic laser process. The classical method of studying each variable at a time can be effective in some cases but it is more expedient to consider combined effects of the process parameters involved [17].

Response surface model (RSM) is a powerful mathematical technique and statistical tool with an assortment of statistical methods by which relations between multiple process variables can be recognized with less experimental tests. It is extensively used as a method of examining and optimizing the operational variables for experimental design, test variables, model development and condition enhancement.

Taguchi's methods generally speed up the experimental process by providing a considerable reduction in the volume of experiments. The choice of the appropriate orthogonal array greatly affects the efficiency of the method [18-22]. Noorul and Jeyapaul [19] adopted orthogonal array, Grey interactive analysis in the ANOVA using Tugachi method to acquire the correct level of identified parameters, and significant correlation of parameters in order for the response efficiency of parameters to be amplified.

In addendum, response surface model was adopted by Palanikumar et al. [23] to improve the efficiency of cutting parameters for surface

roughness by scrutinizing the variance for verification model. Statistical approaches provide instant and reliable short-listing of process conditions, comprehending relations amongst them, and a vast decrease in the overall amount of experiments, this result in the saving of time, chemicals, materials, and manpower. Regardless of the numerous advantages, statistical designs have been applied only to a restrained number of manufacturing processes.

The present work investigates the effects of laser parameters such as laser power, scanning speed and powder feed rate on performance evaluation of alloyed depth and coatings. The overall aim is modelling and optimization of laser alloyed AISI 422 stainless steel using Taguchi approach and response surface model (RSM).

2. MATERIALS AND METHODS

2.1 Materials Preparation

2.1.1 Materials specifications and sample preparation method

The substrate material used in the present investigation was AISI 422 martensitic stainless steel while the reinforcement powder is martensitic stainless steel metal powder (UNS S44004) with the chemical compositions given in Tables 1 and 2. The substrate was cut, and machined into dimensions 100 x 100 x 5 mm^3. Prior to laser treatment, the substrates (X12CrNiMo) were sandblasted, washed, rinsed in water, cleaned with acetone and dried in hot air before exposure to laser beam to minimize reflection of radiation during laser processing and enhance the absorption of the laser beam radiation. Martensitic stainless steel reinforcement metallic powders (TLS Technik GmbH & Co. Bitterfeld, Germany) were used as alloying powder. The particle shape of the powder used was spherical with 45-90 μm particle sizes.

Before characterization of the laser surface alloyed materials, the samples underwent preparation by means of sectioning to rectangles of 15 x 15 mm^2, and clear thermosetting Bakelite resin was used to cold mount them for optical micrographs and black conductive thermosetting resin was utilized for SEM and energy dispersive spectroscopy (EDS) analysis. Specimens for SEM were prepared by cutting samples in such a way to reveal the transverse section of the coatings. The specimens were automatically ground successively using 220, 600, 1000 and 1200 grits SiC papers. They were further polished using polishing cloths and diamond polishing suspensions of 6 to 1 μm to obtain a mirror-like surface. The polished surfaces were rinsed with distilled water and degreased with acetone and dried. Moreover, the substrate specimens were pre-heated to 330°C using a muffle furnace before laser alloying. After laser alloying, the alloyed pre-heated specimen was heated again at 330°C for 1 hour (post-heated) in order to improve the microstructural stability, surface properties through heat treatment.

2.2 Laser Surface Alloying Procedure

Laser surface alloying of the substrate (AISI 422 martensitic stainless steel) with MSS powder (440C) was performed using a 3 kW continuous wave (CW) Ytterbium Laser System (YLS) controlled by a KUKA robot which controls the movement of the nozzle head and emitting a Gaussian beam at 1064 nm. The nozzle was fixed at a distance of 3 mm from the steel substrate. The admixed powders were fed coaxially by employing a commercial powder feeder instrument equipped with a flow balance to control the powder feed rate. Off-axes nozzle fitted onto the Ytterbium fibre laser was used to feed the metallic powder that was simultaneously injected into a melt pool that occurred during scanning of the steel substrate (AISI 422) by means of the laser beam. To inhibit the oxidation of the sample during laser surface alloying, an argon gas at a flow rate of 2.5 L/min was used as the shielding gas. Overlapping the melt tracks at 50% was used to achieve overlapping tracks.

In order to determine the best processing parameters, optimization tests were performed with the laser power of 900-1500 W and scanning speed varied from 0.6 to 1.0 m/min. MSS specimens in form of bars were heated to 330°C using a furnace before laser alloying. The final selection criteria during optimization tests was based on surface having homogeneous layer free of porosity and cracks, all determined from optical microscope (BX51M; Olympus, Ltd) and SEM analysis (JSM-7600F; JOEL, Ltd). The optimum laser parameters used was 1000 W and 1500 W power, 3 mm was the beam diameter, 2.5 L/min gas flow rate, the flow rate of powder was 3.0 g/min and 0.6 m/min and 1.0 m/min were selected as the respective scanning speeds. In order to obtain the optimum laser processing parameters shown in Tables 2 and 3, the laser scanning speeds and constant laser power were altered.

3

2.3 Microstructure of Alloyed Layers

The homogenous distribution of the alloying powder in the melt pool is being assisted by convection flow which subsequently leads to formation of good metallurgical bonding between the powder and the substrate as reported by Popoola and Adebiyi [24]. The depth of the alloyed layer achieved was (1.49 and 0.97 mm) for post-heat specimen, (1.49 and 0.97 mm) for pre-heat specimen and (1.78 and 1.10 mm) for as-received (alloyed without heating) as shown in Fig. 1. The heat affected zone lies between the alloyed zone and the substrate and shows a slightly changed structure compared to the substrate. The shape and depth of these zones depend on the applied laser alloying parameters. It was observed that the heat affected zone was not pronounced, this is attributed to minimal thermal diffusion that took place. Popoola et al. [25] reported enhanced hardness and corrosion properties of pre-heat treatment, post heat treatment of MSS by laser metal deposition. Laser power and scanning speed played important role in the enhanced properties.

2.4 Design of Experiment

Taguchi approach and Response Surface Methodology were used to capture the main effects as well as the interaction effects. The three factors considered are the laser power, scanning speed and powder feed rate. Each of these factors was set at three levels as shown in Tables 3 and 4. The total number of experiments through Taguchi approach is calculated according to equation 1.

$$N = L^F \qquad (1)$$

Where N is the total number of experiments, L is the number of settings or levels, and F is the number of factors. In this research, L=3 and F=3; Hence the total number of experiments according to Taguchi approach is 9. Design Expert 8 and Minitab16 software were used to design and analyse the Taguchi approach and Response Surface Methodology [RSM]. The quality characteristic smaller-the-better, larger-the-better or nominal-the-best has an impact on the method of modelling the S/N ratio [26-29]. The higher the better S/N ratio is adopted in this research.

Higher the better

$$S/N = -10\log\left[\frac{1}{n}\sum_{i=1}^{n}\frac{1}{y_i^2}\right] \qquad (2)$$

Where n is the number of experiments in the orthogonal array and y_i the ith value measured. Table 2 displays the design of the experiment by the input into design Expert 8 and Minilab 16 software. Table 5 is a representation of the design experiment generated by the software.
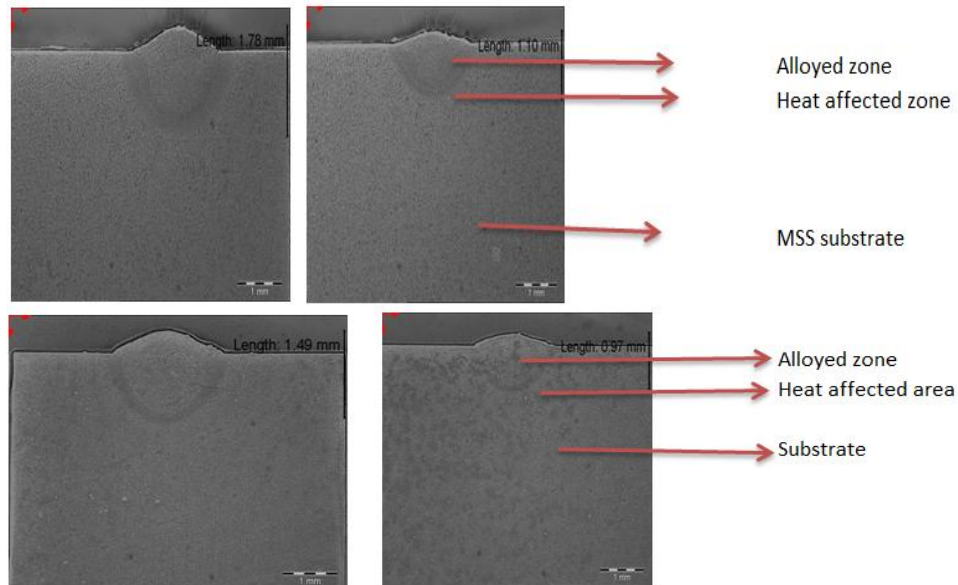

Fig. 1. Stereo micrographs of MSS alloyed specimens at different depth

Table 1. Chemical composition of AISI 422 martensitic stainless steel

Element	Fe	C	Si	Mn	P	Cr	Mo	Ni	V	N_2
Composition (wt %)	Bal.	0.199	0.18	0.65	0.023	11.74	1.32	0.82	0.312	0.0381

Table 2. Chemical composition of martensitic stainless steel powder (UNS S44004)

Element	Fe	C	Mo	Si	Cr	Mn
Composition (wt %)	Bal.	1.02	0.70	0.22	17.41	0.85

Table 3. Laser processing parameters and their levels

Factors	Factors code	Levels		
		1	**2**	**3**
Laser power (kW)	A	1.0	1.25	1.5
Scan speed (m/min)	B	0.6	0.8	1.0
Powder feed rate (g/min)	C	2	3	4

Table 4. Standard L_9 (3^3) orthogonal design

Order	Parameters		
	A	**B**	**C**
1	1	1	1
2	1	2	2
3	1	3	3
4	2	1	2
5	2	2	3
6	2	3	1
7	3	1	3
8	3	2	1
9	3	3	2

3. RESULTS AND DISCUSSION

3.1 Taguchi Approach

The Taguchi optimization technique comprises of the following steps: According to the formula of the higher the better, each S/N ratio can be gotten from observations. The level corresponding to the highest S/N ratio is chosen as the optimum level for each significant level. Through the analysis of variance (ANOVA) of the S/N ratios, a search for the factors that have a considerable impact on the S/N ratio is performed [30,31]. The mean value of alloyed depth for every experimental is shown in Table 5, in addition to the S/N ratios calculated by equation 2. Calculations were performed to establish the average effect of each factor on the quality characteristics at different levels. His

equates to the total of all S/N ratios corresponding to a factor at a specific level divided by the number of repetitions of the factor level [31]. For example, the average S/N ratio of factor A at level 1 is calculated as being

$$([5.01 + 3.464 + 2.734])/3$$

Figs. 4 and 5 show main effect graphs are drawn using the values in Table 6 through Design Expert 6.0.6 statistical software (α=0.05) and Minitab 16 statistical software. Selection for the optimum level is based on the factor levels corresponding to the maximum average effect. Table 6 displays the average factor effect, and Figs. 4 and 5 illustrate the main effects plotted for SNR in each column. Subtraction of the largest value from the smallest value was used to calculate the delta values from Table 4. Adopting the higher the S/N ratio the better strategy led to an optimum condition for alloying. Therefore, $A_2B_1C_1$ was found to be the optimum (Alloyed depth) setting. Table 7 shows a list of corresponding parameter values while the ANOVA is shown in Table 8.

The model is implied to be significant, as attributed to the model F-value of 42.71. Noise gives rise to only a 2.31% chance of a "Model F-Value" being this large. To indicate whether the model terms are significant, the "Prob>F" values should be less than 0.0500. The significant model terms, in this case, are A, B and A^2. Values that are larger than 0.1000 show that the model terms are insignificant. Table 6 displays the standard deviation, R-squared (R^2), Adj R-squared. etc, which are essential for further analysis of the model. The "Pred R-Squared" of 0.8432 is in reasonable agreement with the "Adj R-Squared" of 0.9690. To measure the signal to noise ratio, "Adj Precision" is used. A desirable ratio is one that is greater than 4. In this instance, the Adj Precision ratio is 18.627, which is an indication that the signal/noise ratio is adequate. Hence, it may be concluded that this model is

adequate, and can be used to navigate the design space. Main effects plots of factors can also be used to draw a preliminary conclusion about effects of factors. It can be seen from Figs. 2 and 3 that the alloyed depth decreased by increasing the scanning speed from level 1 to 3 and also peaked at 3.7902 dB at level 2 of

laser power before showing decrease and increase S/N ratios for powder feed rate factor. It can be deduced that increased scanning speed decreases the alloyed depth while S/N ratio of 2.5138 dB was obtained at level 1 of powder feed rate.
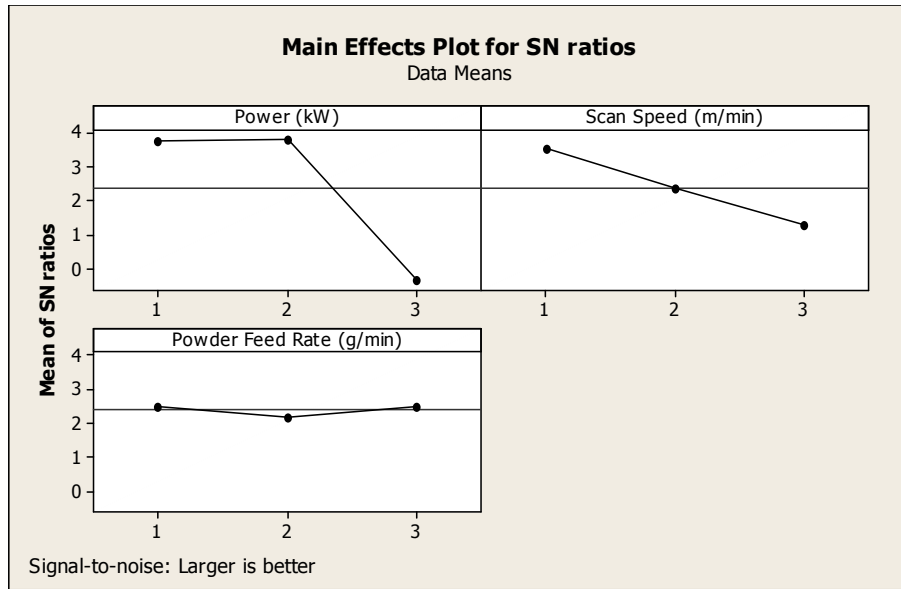

Fig. 2. Main effects plot for S/N ratio

Table 5. L$_9$ orthogonal array matrix for 3 factors with average alloyed depth of experimental results

Standard order	Run order	Laser power (Kw)	Scanning speed (m/min)	Powder feed rate (g/min)	Average alloyed depth (mm)
6	1	1	1	1	1.78
5	2	1	2	2	1.49
1	3	1	3	3	1.37
3	4	2	1	2	1.72
9	5	2	2	3	1.56
8	6	2	3	1	1.38
2	7	3	1	3	1.10
7	8	3	2	1	0.97
4	9	3	3	2	0.83

Table 6. Response table for alloyed depth S/N ratio

Source	Level 1	Level 2	Level 3	Delta	Rank
Laser power	3.7355	**3.7902***	-0.3517	4.1419	1
Scan speed	**3.5156***	2.3539	1.3045	2.2111	2
Powder feed rate	**2.5138***	2.1853	2.4749	0.3285	3

Table 7. Optimum parameters

Factor (Level)	Value
A (2)	Laser power (1.25 kW)
B (1)	Scanning speed (0.6 m/min)
C (1)	Powder feed rate (2 g/min)

Table 8. Analysis of variance (ANOVA) table for the S/N ratio of alloyed depth

Source	SS	DF	MS	*F-Value*	*Prob>F*	% Contibution
Model	0.86	6	0.14	42.71	0.0231	78.79
A	0.68	2	0.34	101.75	0.0097	20.20
B	0.17	2	0.087	26.09	0.0369	0.23
C	0.00202	2	0.00101	0.30	0.7679	0.77
Residual	0.00670	2	0.00334			
Cor total		8				
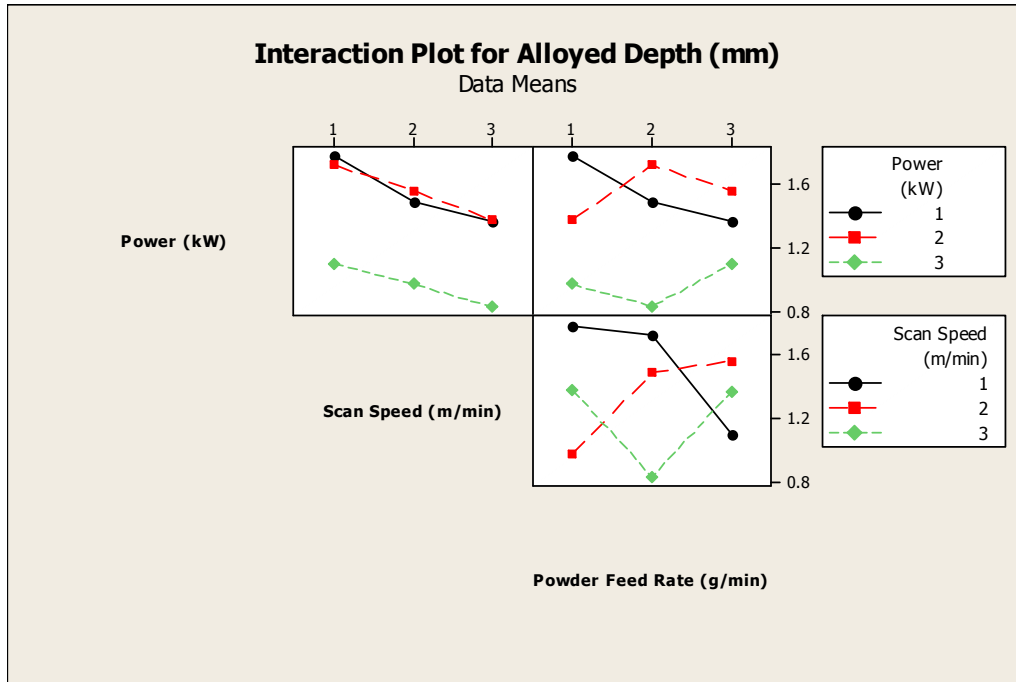
Fig. 3. Interaction plot for alloyed depth

3.1.1 Confirmation experiment

The final step of the design of an experiment is a verification experiment. The purpose is to validate whether the optimum conditions suggested by the matrix experiment do present the improvement projected. A test with optimal setting of the factors and levels formerly assessed is conducted as the verification experiment. Equation 3 is used to calculate the predicted value S/N ratio at the optimum level.

$$\eta = \eta_m + \sum_{i=1}^{j} (\eta_i - \eta_m) \qquad (3)$$

Where j is the number of factors, η_m the mean value of multiple S/N ratios in all experimental runs, and η_i are the multiple S/N ratios corresponding to optimum factor levels [29,32]. From Taguchi's methodology, equation (4) can

be used to predict the alloyed depth obtainable. The S/N ratio calculated for the optimum level is as follows:

$$\eta_0 = \eta_m + (\eta A_2 - \eta_m) + (\eta B_1 - \eta_m) + (\eta C_1 - \eta_m) \quad (4)$$

Where η_0 is the optimum S/N ratio, and η_m the overall mean of S/N values, ηA_2 the average value of S/N at the second level of laser power, ηB_1 the average value of S/N at the first level of scanning speed and ηC_1 is the average value of S/N at the first level of powder feed rate. Substituting the values of various terms in equation (4),

$$\eta_0 = 2.391 + (3.790 - 2.391) + (3.516 - 2.391) + (2.514 - 2.391) = 5.037 dB.$$

If the S/N ratio is known and we want to learn about the expected result that will make the S/N, the procedure is to back-transform S/N to find the performance value expected [28,33]. When the value 5.037dB is placed into equation 2, the value of alloyed depth obtained is 1.786 mm. Alloyed depth of other combinations can be derived using the same formula. To check the optimum results obtained through Taguchi's method, confirmation trials are carried out and the results are tabulated in Table 9 for alloyed depth. From the table it is clearer that the predicted conditions for higher alloyed depth suits well with the experimental results. Furthermore, the optimum design ($A_2B_1C_1$) was laser alloyed and the alloyed depth of the MSS was measured three times and the average of the results was determined as 1.775 mm which corresponds to 4.982dB (Table 9). This result is very close to that estimated by Taguchi design (1.786 mm/5.037 dB). The initial design is accepted as $A_1B_1C_1$ then the S/N ratio is also obtained. As seen in Tables 9, the improvement in the alloyed depth at the optimum level is found to be 0.011 mm. The difference between the predicted value from Taguchi of Minitab software version 16 and the values determined by the experiment at the feasible optimal condition is 0.026 mm. This demonstrates that Taguchi model is a suitable tool to predict alloyed depth.

Table 9. Results of optimum and initial design for alloyed depth

Design	Taguchi prediction (mm)	Experimental verification (mm)
Initial design ($A_1B_1C_1$)	1.775	1.740
Optimum design ($A_2B_1C_1$)	1.786	1.760
Gain	0.011	0.020

3.2 Response Surface Model

Response surface model (RSM) is usually considered in the context of experimental design as a statistical method for modelling and analyzing of problems in which different variables affect a response of interest. The RSM field comprises of the experimental approach for exploring the space of the process or independent variables, statistical modelling that is empirical to create a fitting approximating correlation between the yield and the process variables, and optimization methods for finding the values of process variables that give the

required values of the response [34]. The main objective of RSM is to find the combination of factor levels to achieve the optimal response. In the present work, the RSM is used to study the effects of process variables on laser alloyed depth quality. The result of experiment is used to develop the regression model by establishing a correlation between the process control parameters and laser alloyed depth.

3.2.1 Numerical analysis for the response surface model

In design expert 8 environments, the software presents the summary of different models and the appropriate model was suggested. The design summary presented shows the model type and the important properties, such as the P-value for the lack of fit, the adjusted R-squared and predicted R-squared values, which are important for model evaluation and development. The first step in the model building is to select the appropriate model, and the model is analysed. The appropriate model selected in this research work is a quadratic model (Linear and squared) because it has better properties than any of the other types. A quadratic regression model is developed for alloyed depth founded on experimental findings utilizing MINITAB software of version 16.0 and Design Expert software of version 8.0. The response as a function of independent variables and their interactions was predicted with the aid of the model. Figs. 5 and 6 graphically show the effects of scan speed, laser power and powder feed rate on alloyed depth by constructing the response surface and contour diagrams. A second-order response surface model equation is as follows [35]:

$$Y_u = \beta_0 + \sum_{i=1}^{n} \beta_i x_{iu} + \sum_{i=1}^{n} \beta_{ii} x_{iu}^2 + \sum_{i<j}^{n} \beta_{ij} x_{iu} x_{ju} + \varepsilon \quad (5)$$

Where Y_u is the predicted response, β_0 the intercept coefficient, β_1 the linear terms, β_{ii} the squared terms, β_{ij} the interaction terms, x_{iu} and x_{ju} are coded levels of the process control variables, the residual, ε measures the experimental error of the $u-th$ observation and n is the total number of designed variables [36,37]. The coefficients of the model for the corresponding response are estimated using regression analysis technique included in RSM. The response surface of alloyed depth can be

expressed by the following quadratic equation in terms of coded factors.

Alloyed Depth (mm) =
$$1.53 - 0.29\,A - 0.17\,B - 0.02\,C - 0.3\,A^2 \quad (6)$$
$$+ 0.02\,B^2 + 0.01\,C^2$$

Where, A is Laser Power (kW), B is Scan Speed (m/min) and C is the Powder Feed rate (g/min). As shown in equation 6, quadratic model is the most suited mathematical method for predicting laser alloyed depth, with Table 10 displaying the full regression ANOVA table for alloyed depth.

Table 10 shows the ANOVA table for regression analysis. Analysis of variance (ANOVA) is used for evaluating the effects of parameters on the process. ANOVA finds the significant factor effects based on the desired confidence interval. This table indicates that the model estimated by regression procedure is significant at the α-level of 0.05 [38]. In this table DF is the degree of freedom, SS the sequential sum, MS mean squares, F the F-value, P the P-value. So the P-values, which are less than 0.05 indicate the significance of each respective factor. Laser power and Scan speed are more significant and contributed more in the regression model for alloyed depth. Regression analysis is performed to find out the relationship between factors and alloyed depth. Accordingly, a second order polynomial best predicts the observation. The regression equation in terms of factors (Table 2) is obtained and presented as R^2 (=$SS_{Regression}/SS_{Total}$) and R^2_{adj}.

Statistical analyses are used to assess the best order of the polynomial. R^2 indicates how well the model fits the data. These values are calculable for different orders of regression equations. Predicted R^2 and R^2_{adj} are 0.9923 and 0.969,

respectively. Larger values of predicted R^2 suggest models of greater predictive ability.

The model F-value of 42.71 implies the model is significant. There is only a 2.31% chance that a "Model F-Value" this large could occur due to noise. Values of "Prob>F" less than 0.0500 indicate model terms are significant. In this case A, B and A^2 are significant model terms. Values greater than 0.1000 indicate the model terms are not significant. Table 8 shows the standard deviation, R-squared (R^2) and $R^2_{adjusted}$ which are important for further analysis of the model. The "Pred R-Squared" of 0.8432 is in reasonable agreement with the "Adj R-Squared" of 0.9690. "Adj Precision" measures the signal to noise ratio. A ratio greater than than 4 is desirable. In this case, the Adeq Precision ratio is 18.627 which indicate an adequate signal/noise ratio. It may therefore be concluded that this model is adequate, and could be used to navigate the design space. The Final equation in terms of coded factors is shown in equation 5.
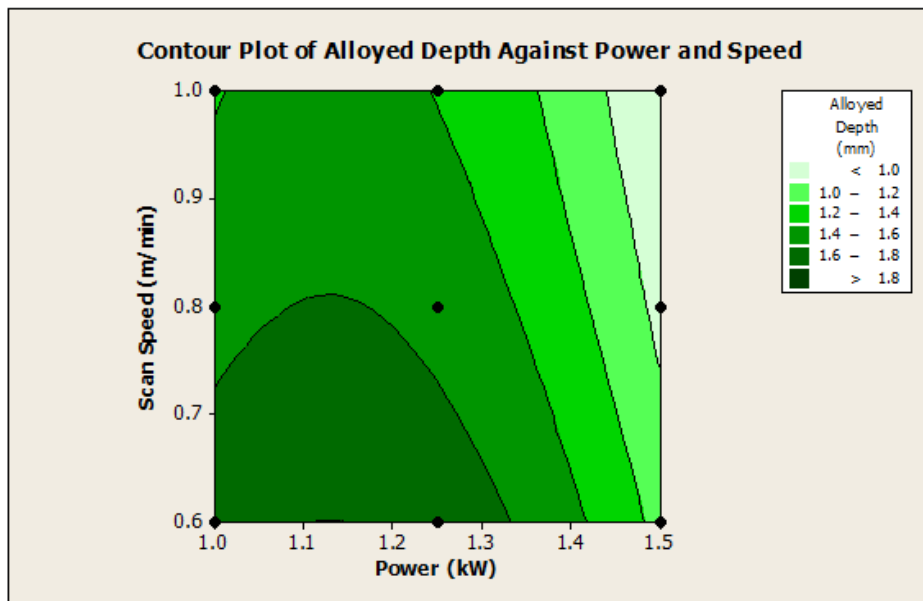
The surface and contour plots of the interactions between laser power, scanning speed and powder feed rate are shown in Figs. 4(a-b). The surface and contour plots of laser power and scanning speed showed a very strong interaction between them. At high laser power and low scanning speed of 0.6 m/min, the alloyed depth produced is 1.72 mm. This is because at high laser power and low scanning speed there is sufficient power and interaction time of the laser and material to properly melt the powder and produce better surface finish. On the hand, at low laser power, the alloyed depth decreases with increased scanning speed. This is due to insufficient laser material interaction time. The surface and contour plots are shown in Figs. 4 and 5.

Table 10. ANOVA regression analysis

| Source	DF	Seq SS	Adj SS	Adj MS	*F*	*P*
Regression	6	0.857133	0.857133	0.142856	42.71	0.0023
Linear	3	0.679667	0.679667	0.226556	67.74	0.015
A	**1**	**0.504600**	**0.504600**	**0.504600**	**150.88**	**0.007**
B	**1**	**0.173400**	**0.173400**	**0.173400**	**51.85**	**0.019**
C	1	0.001667	0.001667	0.001667	0.50	0.553
Square	3	0.177467	0.177467	0.059156	17.69	0.054
A^2	**1**	**0.176022**	**0.176022**	**0.176022**	**52.63**	**0.018**
B^2	1	0.001089	0.001089	0.001089	0.33	0.626
C^2	1	0.000356	0.000356	0.000356	0.11	0.775
Residual	2	0.006689	0.006689	0.003344		
Total	8	0.863822				
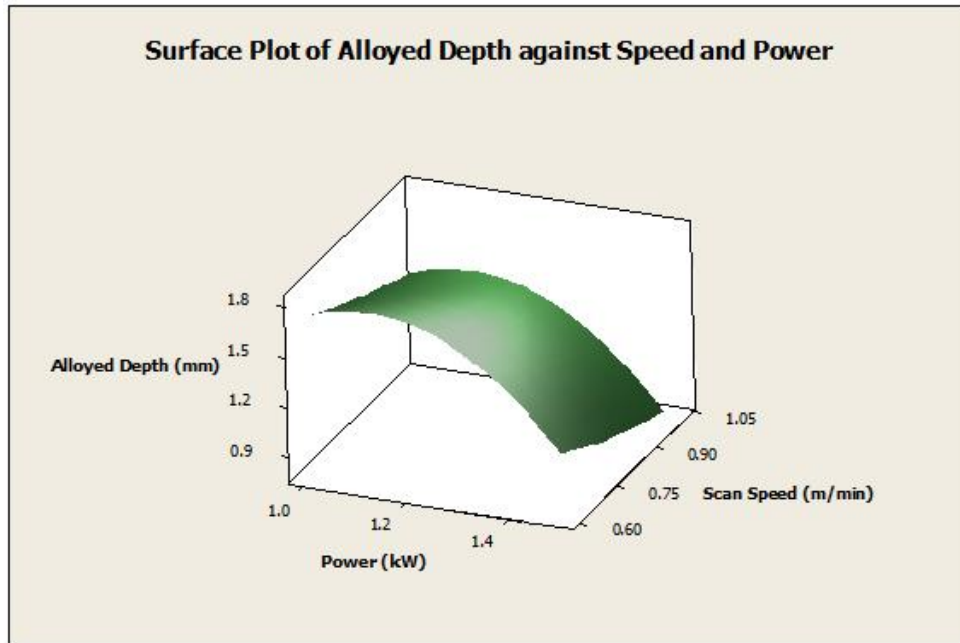
a

b

Fig. 4(a-b). Surface and contour plots of alloyed depth against laser power and scan speed

A similar interaction is also observed in the surface and contour plots of laser power and powder feed rate in Fig. 5(a-b). The high alloyed depth observed at high laser power and low powder feed rate was as a result of sufficient laser power for the available powder which resulted in the proper melting of the MSS substrate. While at low laser power and high powder feed rate there was decrease in alloyed depth due to insufficient laser powder to properly melt the high volume of powder delivered into the melt pool. Moreover, increased scanning speed and powder feed rate resulted in decreased alloyed depth as shown in Fig. 6(a-b). At low

scanning speed and low powder feed rate, alloyed depth was high. Whereas, at high scanning speed and high powder feed rate, the volume of powdered delivered to the melt pool was higher and the laser material interaction times was low making it impossible for proper melting.
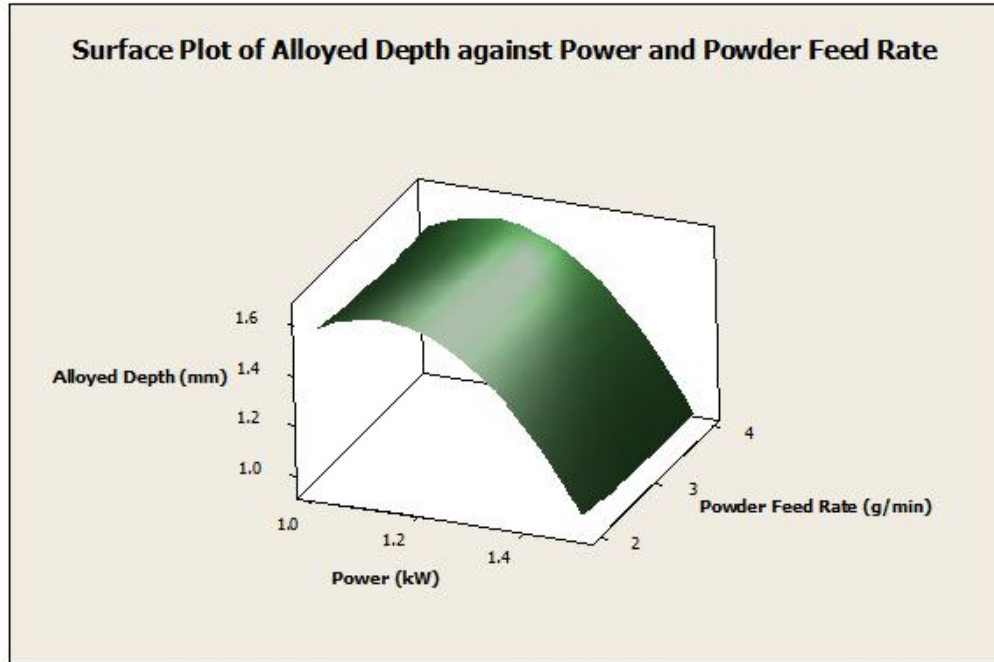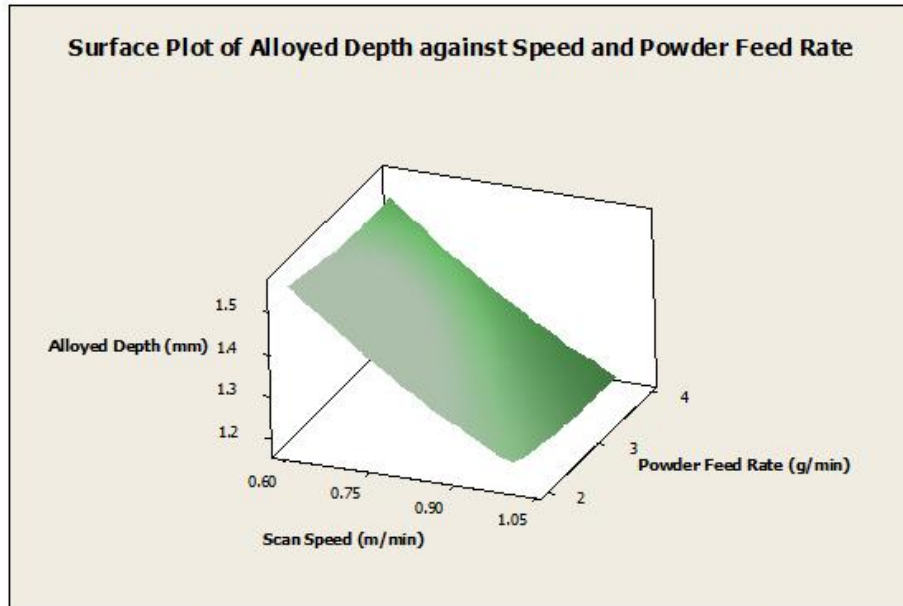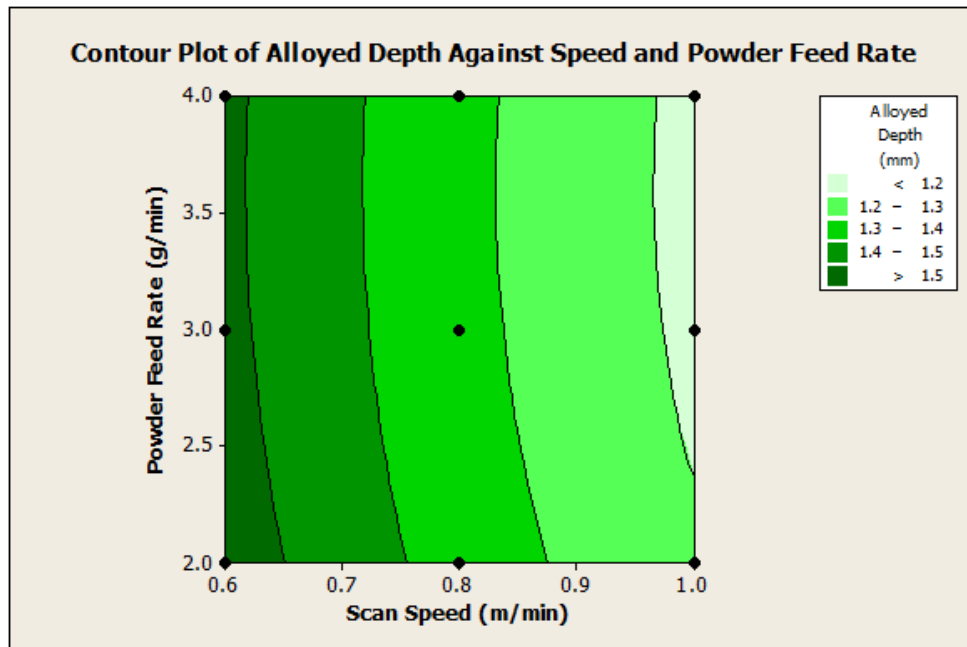

a
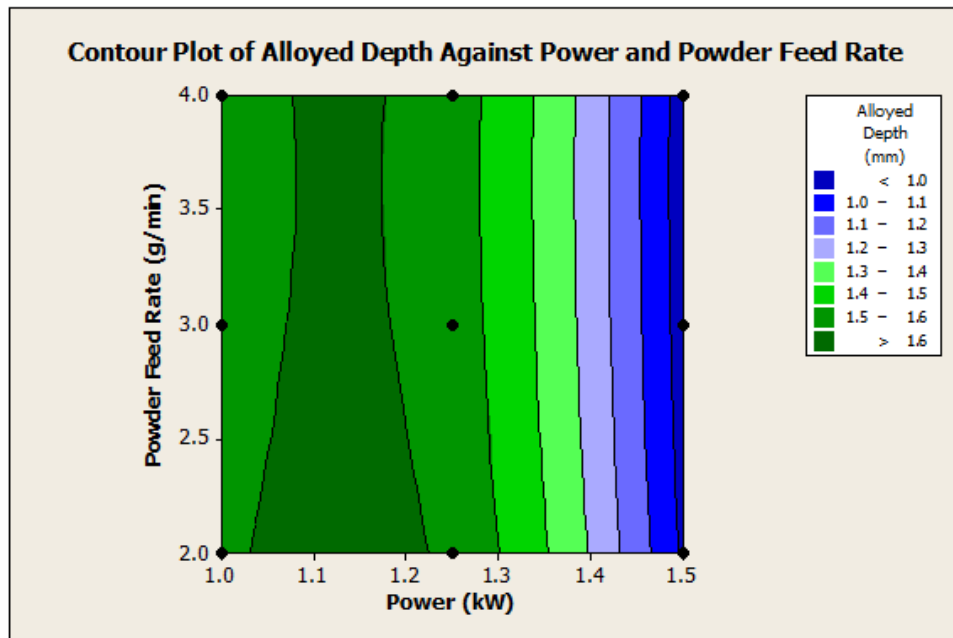
b

Fig. 5(a-b). Surface and contour plots of alloyed depth against laser power and powder feed rate

a

b

Fig. 6(a-b). Surface and contour plots of alloyed depth against speed and powder feed rate

Response Optimizer function of Minitab Software 16 was used to obtain the response optimization plot for laser alloying process parameters, as it can be seen from Fig. 7. Desirability function was selected to find suitable value of the factors. It is observed from this figure that the objective optimization of the response (alloyed depth) was achieved at laser power of 1.1263 kW, scan speed of 0.6 m/min and powder feed rate of 2.0 g/min. Therefore, it can be concluded that the

alloyed depth during laser alloying process can effectively be predicted by the proposed empirical models (Taguchi model and RSM) and this is shown in Table 11.

It is necessary to check the adequacy of the fitted model to ensure that it provides a tolerable approximation to the real system. Proceeding with optimization of the fitted response surface model without an adequate fit may give misleading results. In judging of the model adequacy, the residuals from the least square method play a crucial role. A check is made by constructing a normal probability plot of the residuals as shown in Fig. 8a. The normality assumption is satisfied as the residual plot approximated along a straight line. Fig. 8b represents a residual versus predicted response plot. It is observed that residuals scatter

randomly on the display, indicating that the variance of the original observation is constant for all values of response. The residual plot also shows how the error between the actual response and the predicted response of the model is distributed. It also gives an indication of how well the selected model fits. Studentized residual obtained by dividing the residual by an estimate of its standard deviation. This is a kind of data normalization process that helps in detecting outliers. The normal residuals plot shows that the residuals are normally distributed. The externally studentized residual also shows that the residuals are within the red lines, which indicates that there is no outlier. Both plots (Figs. 8a and 8b) are satisfactory, so it can be deduced that the developed mathematical model is good enough to describe the laser alloyed depth by response surface methodology.

Table 11. Comparison of Alloyed Depths Predicted by Taguchi model and RSM

Response	Taguchi	RSM	Experimental
Alloyed depth (mm)	1.7859	1.8231	1.760
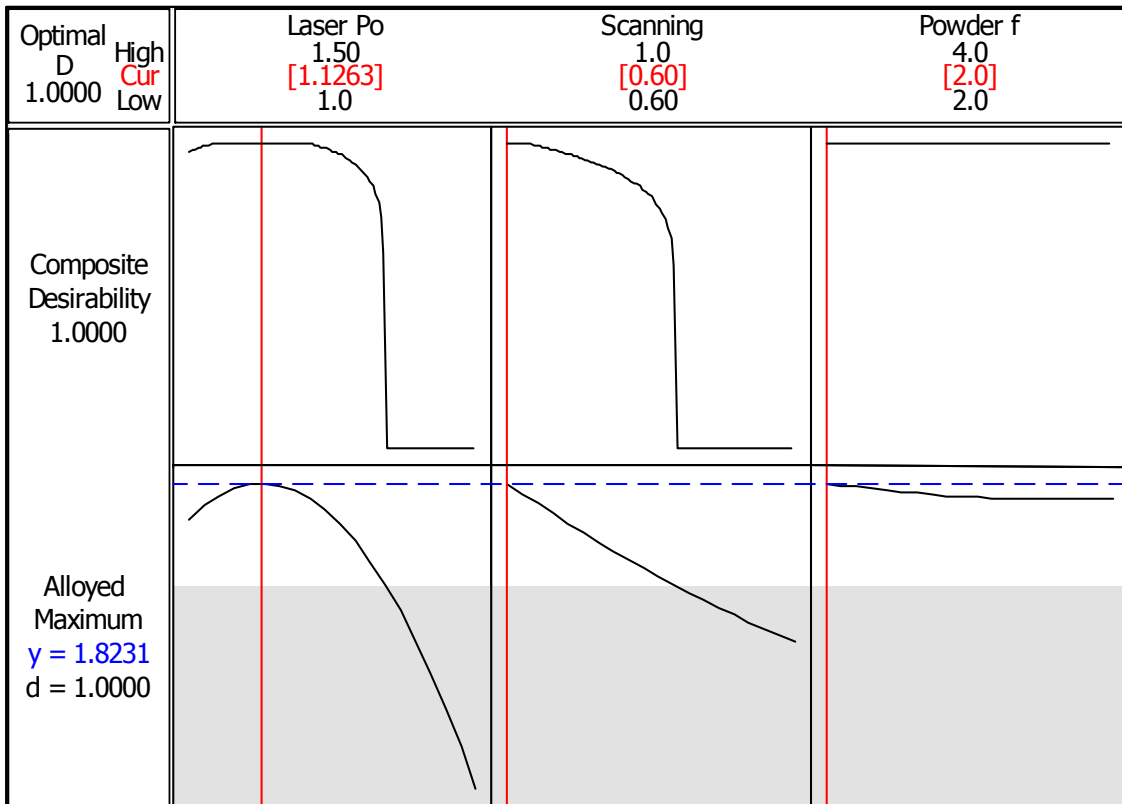
Fig. 7. Response optimization plot for laser alloying process parameters
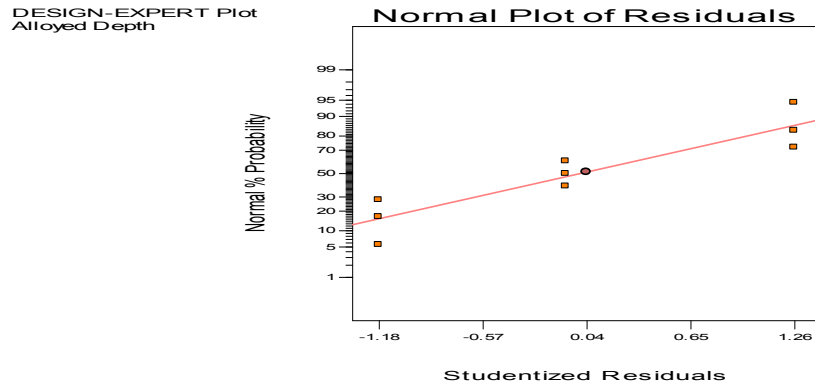
13

Fig. 8a. Plot of normal percentage probability versus internally studentized residuals
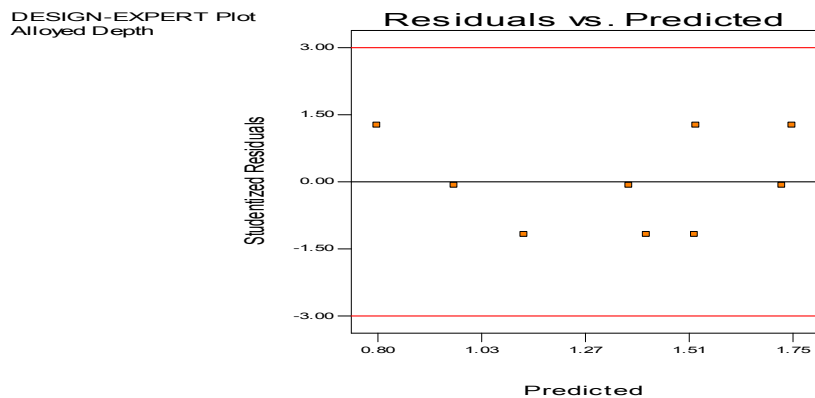

Fig. 8b. Plot of internally studentized residuals versus predicted response

4. CONCLUSION

This research presents the Taguchi approach and response surface model (RSM) for optimization of alloyed depth in laser alloyed matensitic stainless steel. The influence of laser parameters on alloyed depth has been examined. Methods used for experimentation were Taguchi technique, ANOVA and response surface model (RSM). From the experimental findings and derived analysis, it can be concluded that:

❖ Well optimized process parameters and carefully chosen reinforcement materials fractions produced quality coatings. High residual stresses and crack formation was eliminated through optimization of laser processing parameters, leading to enhanced quality of the coatings, surface adhesion between substrate and reinforcement materials, and micro-structural evolution.

❖ Laser power and scanning speed have most significant influence on alloyed depth while powder feed rate has minimal effect.

❖ The correlation between factors and alloyed depth was derived using a regression analysis and an optimum parameter combination for the maximum alloyed depth was obtained by using the analysis of signal-to-noise (*S/N*) ratios.

❖ It was observed from both Taguchi model and RSM that the laser power could be kept at 1.25 kW and 1.1263 kW respectively, scanning speed at 0.6 m/min, while the powder feed rate should be kept at 2 g/min for optimum and quality alloyed depth.

❖ The response surface and Taguchi models developed show that a predictive model could be employed to determine the influence of processing parameters on the alloy depth alloyed of MSS for engineering applications. The predictive model developed served as a powerful tool used for the effective control of the process, and the achievement of desired component's properties.

COMPETING INTERESTS

Authors have declared that no competing interests exist.

REFERENCES

1. Yetim AF, Yildiz F, Vangolu Y, Alsaran A, Celik A. Several plasma diffusion processes for improving wear properties of Ti6Al4V alloy. Wear. 2009;267:2179-2185.

2. Mahmoudi B, Torkamany MJ, Aghdam AR, Sabbaghzade J. Laser surface hardening of ISI 420 stainless steel treated by pulsed Nd:YAG Laser. Materials and Design. 2010;31:2553-2560.

3. Singh S, Nanda T. Effect of alloying and heat treatment on the properties of super martensitic stainless steels. International Journal of Engineering Technology and Scientific Research. 2010;1(1):1-4.

4. Callister WD. Material science and engineering. Sedriks Wiley & Sons, Inc., 7th ed. 2007;343-345.

5. Peyre P, Chaieb I, Braham C. FEM calculation of residual stresses induced by Laser Shock processing in stainless steels. Modelling and Simulation in Materials Science and Engineering. 2007;15:205-221.

6. Alexandre VLB, Davis ML, Frederico PF, Luiz CC, Pedro APN. Surface modification of the AISI 410 martensitic stainless steel by plasma nitriding; 2009.

7. Lo KH, Cheng FT, Man HC. Laser transformation hardening of AISI 440C martensitic stainless steel for higher cativation erosion resistance. Surface and Coatings Technology. 2003;173:96-104.

8. Lo KH, Kwok CT, Cheng FT, Man HC. Effects of laser treatments on cativation erosion and corrosion resistance of AISI 440C martensitic stainless steel. Materials Letters. 2003;58:88-93.

9. Xi YT, Liu DX, Han D. Improvement of corrosion and wear resistances of AISI 420 martensitic stainless steel using plasma nitriding at low temperature. Surface and Coatings Technology. 2008;202:2577-2583.

10. Lo KH, Cheng FT, Man HC. Improvement of cativation erosion resistance of AISI 440C martensitic stainless steel by laser surface alloying using fine WC powder. Surface and Coatings Technology. 2003; 165:258-267.

11. Barlow LD, Du Toit M. Effect of austenitizing heat treatment on the microstructure and hardness of martensitic stainless steel AISI 420. 2011;21:1327-1336.

12. Abdolahi A, Shahverdi HR, Torkamany MJ, Emami M. Improvement of the corrosion behaviour of low carbon steel by laser surface alloying. Applied Surface Sciences. 2011;257:9921-9924.

13. Lo KH, Kwok CT, Cheng FT, Man HC. Effects of laser treatments on cativation erosion and corrosion resistance of AISI 440C martensitic stainless steel. Materials Letters. 2003;58:88-93.

14. Kwok CT, Lo KH, Cheng FT, Man HC. Cativation erosion and pitting corrosion behaviours of laser-melted martensitic stainless steel UNS S42000. Surface and Coatings Technology. 2000;126:238-255.

15. Zhang Q, Yao J, Wang L, Kong F, Lou C, Chen Z. Surface laser alloying of 17-4PH stainless steel steam turbine blades. Optics and Laser Technology. 2008;40: 838-843.

16. Kwok CT, Lo KH, Cheng FT, Man HC. Cativation erosion and corrosion behaviours of laser-aluminized mild steel. Surface and Coatings Technology. 2006; 166:221-230.

17. Karuppaiya M, Sasikumar E, Viruthagiri T, Vijayagopal V. Optimization of process conditions using response surface methodology for ethanol production from waste cashew apple juice by Zymomonas mobilis. Chemical Engineering Communication. 2009;196: 1425-1435.

18. Thamizhmanil S, Saparudin S, Hasan S. Analyses of surface roughness by turning process using Taguchi Method. Journal of Achievements in Materials and Manufacturing Engineering. 2007;20:503-505.

19. Noorul HA, Marimuthu P, Jeyapaul R. Multi-response optimization of machining parameters of drilling Al/SiC metal matrix composite using grey relational analysis in the Taguchi Method. International Journal of Advanced Manufacturing Technology. 2007;250-255.

20. Rossella S, Luigi A, Antonio D, Giancarlo B. Application of Taguchi method for the multi-objective optimization of aluminium foam manufacturing parameters. International Journal of Material Forming; 2009.

21. Tosun N, Ozler L. Optimization for hot turning operations with multiple performance characteristics. International Journal of Advanced Manufacturing Technology. 2004;3:777-782.
22. Lin TR. Experimental design and performance analysis of TiN-coated carbide tool in face milling stainless steel. Journal of Materials Processing Technology. 2002;127:1-7.
23. Palanikumar K, Shanmugam K, Paulo DJ. Analysis and optimization of cutting parameters for surface roughness in machining Al/SiC particulate composites by PCD tool. International Journal of Materials and Product Technology. 2010; 37:117-128.
24. Popoola API, Fatoba OS, Popoola OM, Pityana SL. The Influence of heat treatment and process parameter optimization on hardness and corrosion properties of laser alloyed X12CrNiMo steel. Silicon. 2016;8(4):579-589.
25. Fatoba OS, Popoola API, Aigbodion VS. Experimental study of hardness values and corrosion behaviour of laser alloyed Zn-Sn-Ti coatings of UNS G10150 mild steel. Journal of Alloys and Compounds. 2016; 658:248-254.
26. Park CK, Ha JY. A process for optimizing sewing conditions to minimize seam pucker using the Taguchi method. Textile Research Journal. 2005;75(3):245-252.
27. Taguchi G, Chowdhury S, Wu Y. Taguchi's quality engineering handbook. John Wiley &Sons, Inc. 2005;1662.
    ISBN: 0-471-41334-8
28. Roy RK. Design of experiment using Taguchi approach. A Wiley-interscience Publication. 2001;538.
    ISBN: 0-471-36101-1
29. Ross PJ. Taguchi techniques for quality engineering. Mcgraw-Hill International Editions. 1996;329.
    ISBN: 0-07-114663-6
30. Mel M, Karim MIA, Jamal P, Salleh MRM, Zakaria RA. The influence of process parameters on lactic acid fermentation in laboratory scale fermenter. Journal of Applied Sciences. 2006;6(10):2287-2291.
31. Chen QH, Au KF, Yuen CWM, Yeung KW. Effects of yam and knitting parameters on the spirality of cotton single jersey fabrics. Textile Research Journal. 2003;73(5):421-426.
32. Dubey AK, Yadava V. Simultaneous optimization of multiple quality characteristics in laser beam cutting using Taguchi method. International Journal of Precision Engineering and Manufacturing. 2007;8(4):10-15.
33. Savaskan M. Comparative analysis of design of experiment techniques on the performance evaluation and optimization of hard ceramic coated drill bits. Ph.D. Thesis. Istanbul Technical University, Institute of Natural and Applied Science. 2003;277.
34. Acherjee B, Dipten Mistra DB, Venkadeshwaran K. Prediction of weld strength and seam width for laser transmission welding of thermoplastic using response surface methodology. Optics and Laser Technology. 2009;41: 956-967.
35. Subrata M, Asish B, Pradip K. Ni-Cr-Mo cladding on mild steel surface using CO_2 laser and process modelling with response surface methodology. International Journal of Engineering Science and Technology. 2011;3(8):6805-6816.
36. Montgomery DC. Design and analysis of experiments. 5th edition. New York: Wiley; 2001.
37. Jiang-Ping W, Yong-Zhen C, Xue-Wu G, Han-Qing Y. Optimization of coagulation-flocculation process for a paper-recycling wastewater treatment using response surface methodology. Colloids and Surfaces A. 2007;302:204-210.
38. Bala MG, Biswanath M, Sukamal G. Taguchi method and ANOVA: An approach for process parameters optimization of hard machining while machining hardened steel. Journal of Scientific and Industrial Research. 2009;68:686-695.

Peer-review history:
The peer review history for this paper can be accessed here:
http://sciencedomain.org/review-history/20791